

Transport Reversible Jump Markov Chain Monte Carlo with proposals generated by Variational Inference with Normalizing Flows

Pingping Yin¹ Xiyun Jiao¹

Abstract

We present a framework using variational inference with normalizing flows (VI-NFs) to generate proposals of reversible jump Markov chain Monte Carlo (RJMCMC) for efficient trans-dimensional Bayesian inference. Unlike transport reversible jump methods relying on forward KL minimization with pilot MCMC samples, our approach minimizes the reverse KL divergence which requires only samples from a base distribution, eliminating costly target sampling. The method employs RealNVP-based flows to learn model-specific transport maps, enabling construction of both between-model and within-model proposals. Our framework provides accurate marginal likelihood estimates from the variational approximation. This facilitates efficient model comparison and proposal adaptation in RJMCMC. Experiments on illustrative example, factor analysis and variable selection tasks in linear regression show that TRJ designed by VI-NFs achieves faster mixing and more efficient model space exploration compared to existing baselines. The proposed algorithm can be extended to conditional flows for amortized variational inference across models. Code is available at https://github.com/YinPingping111/TRJ_VINFs.

1. Introduction

Bayesian statistics makes inference based on Bayes’ theorem. For a given model $\pi(\mathbf{y} \mid \boldsymbol{\theta}_k, k)$ indexed by model k and parameter vector $\boldsymbol{\theta}_k \in \mathbb{R}^{n_k}$, the joint posterior distribution over models and parameters is given by

$$\pi(k, \boldsymbol{\theta}_k \mid \mathbf{y}) \propto \pi(k) \pi(\boldsymbol{\theta}_k \mid k) \pi(\mathbf{y} \mid \boldsymbol{\theta}_k, k),$$

where $\pi(k)$ is the prior probability of model k , $\pi(\boldsymbol{\theta}_k \mid k)$ is the prior over parameters under model k , and $\pi(\mathbf{y} \mid \boldsymbol{\theta}_k, k)$

¹Department of Statistics and Data Science, Southern University of Science and Technology, Shenzhen, China. Correspondence to: Xiyun Jiao <jiaoxiy@sustech.edu.cn>.

is the likelihood. Since the dimension n_k of $\boldsymbol{\theta}_k$ may differ across models, the inference task considered here involves a trans-dimensional probability distribution with support

$$\mathcal{X} = \bigcup_{k \in \mathcal{K}} (\{k\} \times \Theta_k),$$

a space arise naturally in many Bayesian model inference problems, such as Bayesian model determination (Lopes & West, 2004), variable selection (Jasra et al., 2007), phylogenetic tree topology search (Jiao et al., 2021), mixture components inference (Pravitasari et al., 2019), change-point models (GREEN, 1995), etc.

1.1. Reversible Jump Markov Chain Monte Carlo

The problem of interest is sampling from a probability distribution defined on a trans-dimensional space. However, since Θ is a union of spaces of different dimensions, measure-theoretic subtleties prevent the direct use of classic algorithms such as Metropolis–Hastings (MH) (Hastings, 1970). Reversible Jump Markov Chain Monte Carlo (RJMCMC), first introduced by GREEN (1995), is a generalized MH algorithm based on a mixture of kernels. It alternates between “within-model” kernels—standard moves that stay in the same model—and “between-models” kernels, which propose transitions from $\{k \times \Theta_k\}$ to $\{k' \times \Theta_{k'}\}$.

Trans-dimensional moves are implemented as follows. First, a new model index k' is sampled from $q(k' \mid k)$. Then, a move must be proposed between Θ_k and $\Theta_{k'}$, which generally have different dimensions n_k and $n_{k'}$. The core idea of RJMCMC is to extend the spaces with auxiliary variables to achieve dimension matching. Specifically, we introduce $\mathbf{u}_{k,k'}$ and $\mathbf{u}_{k',k}$ with distributions $\varphi_{k,k'}$ and $\varphi_{k',k}$, respectively, such that $n_k + \dim(\mathbf{u}_{k,k'}) = n_{k'} + \dim(\mathbf{u}_{k',k})$. Given $\boldsymbol{\theta}_k$, we sample $\mathbf{u}_{k,k'} \sim \varphi_{k,k'}$ and apply a deterministic diffeomorphism $(\boldsymbol{\theta}_{k'}, \mathbf{u}_{k',k}) = h_{k,k'}(\boldsymbol{\theta}_k, \mathbf{u}_{k,k'})$, where the distributions φ are arbitrary and $h_{k,k'}$ must be invertible and differentiable. Let $\mathbf{x} = (k, \boldsymbol{\theta}_k)$ and $\mathbf{x}' = (k', \boldsymbol{\theta}_{k'})$. Following the Metropolis-Hastings framework and enforcing detailed balance, the RJMCMC acceptance probability is:

$$\alpha(\mathbf{x}, \mathbf{x}') = \min \left(1, \frac{\pi(\mathbf{x}' \mid \mathbf{y}) \varphi_{k',k}(\mathbf{u}_{k',k})}{\pi(\mathbf{x} \mid \mathbf{y}) \varphi_{k,k'}(\mathbf{u}_{k,k'})} \cdot \frac{q(k \mid k')}{q(k' \mid k)} \cdot J_{k,k'} \right),$$

where

$$J_{k,k'} = \left| \frac{\partial h_{k,k'}(\boldsymbol{\theta}_k, \mathbf{u}_{k,k'})}{\partial (\boldsymbol{\theta}_k, \mathbf{u}_{k,k'})} \right|.$$

Improving trans-dimensional proposal mechanisms has been a central focus in RJMCMC research. Brooks et al. (2003) developed theoretical guidelines via Taylor series expansions of acceptance probabilities, connecting to Langevin-type updates and saturated space approaches. Green & Mira (2001) introduced delayed rejection mechanisms, allowing adaptive re-proposals to reduce persistent rejection. Jasra et al. (2007) extended population-based MCMC to trans-dimensional settings using parallel tempering for improved exploration. For automated proposal construction, Fan et al. (2009) employed marginal density estimators, while Karagiannis & Andrieu (2013) bridged models via annealed importance sampling with intermediate tempering steps. Gagnon (2021) leveraged asymptotic approximations to achieve near-optimal large-sample performance. Davies et al. (2023) first applied non-linear transport maps via normalizing flows trained by forward KL divergence to construct proposals between models with complex dependency structures.

1.2. Variational Inference with Normalizing Flows

VI is an optimization-based approach to approximating distributions (Blei et al., 2017). VI searches for the optimal distribution that minimizes the distance (typically measured by the Kullback–Leibler (KL) divergence) to the target posterior from a set of tractable distributions. Compared to MCMC, VI is much less expensive in computation and much more scalable with dimension. However, VI can introduce significant bias if all the distributions in the candidate family are far away from the target distribution. Rezende & Mohamed (2015) introduce a new approach for specifying flexible, arbitrarily complex and scalable approximate posterior distributions, where the approximations are distributions constructed through a normalizing flow. A normalizing flow describes the transformation of a probability density through a sequence of invertible mappings. By repeatedly applying the rule for change of variables, the initial density ‘flows’ through the sequence of invertible mappings. At the end of this sequence we obtain a valid probability distribution and hence this type of flow is referred to as a normalizing flow. There has been much recent work on normalizing flows, ranging from improving their expressive power to expanding their application (Papamakarios et al., 2021). Examples of work using flows in variational inference are given by Dinh et al. (2017); Kingma et al. (2016); Rezende & Mohamed (2015); Tomczak & Welling (2016); Stimper et al. (2023); Durkan et al. (2020); Andrade (2024); Wu & Xie (2025)

1.3. Transport MCMC and Transport RJMCMC

When the geometry of the target distribution is unfavorable, Markov Chain may take many evaluations of the log-probability of the target distribution and its gradient for the chain to mix between distant state (Neal, 2011). To address this issue, several transport-based methods have been proposed. Marzouk et al. (2016); Parno & Marzouk (2018) presented the fundamentals of a measure transport approach to sampling, and first introduced an approach that adaptively constructs a lower-triangular transport map using information from previous MCMC states. By applying deterministic couplings, they transform classical Metropolis proposals—such as random walk or Langevin dynamics—into non-Gaussian proposal distributions capable of more efficiently exploring the target density. Subsequently, Hoffman et al. (2019) proposed Neural Transport (NeuTra) Hamiltonian Monte Carlo (HMC), which employs inverse autoregressive flows (IAF) (Kingma et al., 2016) to correct unfavorable geometry in HMC (Neal, 2011). South et al. (2019) developed Annealed Flow Transport (AFT), a method combining Annealed Importance Sampling and Sequential Monte Carlo, in which normalizing flows are learned sequentially to guide particles toward annealed target distributions. More recently, Gabri e et al. (2021) utilized the forward KL divergence as a training objective, where samples from the posterior are generated via a local MCMC algorithm enhanced by a normalizing flow, thereby accelerating mixing; these samples are then used to train the flow. However, a limitation of such approaches is their reliance on prior knowledge of mode locations in multimodal distributions. Finally, Davies et al. (2023) extended measure transport to design cross-model proposals in reversible jump MCMC, yielding the Transport Reversible Jump (TRJ) method.

The transport reversible jump (TRJ) method (Davies et al., 2023) provides a systematic framework for constructing trans-dimensional proposals by leveraging approximate transport maps. Building upon the mathematical foundation of transport theory, where a transport map $T : \mathbb{R}^n \rightarrow \mathbb{R}^n$ satisfies $\mu_z = T_{\#} \mu_{\theta}$ for distributions μ_{θ} and μ_z , TRJ extends this concept to model selection scenarios. Let ν be a univariate analytic reference distribution (e.g., standard Gaussian). For each model $k \in \mathcal{K}$, we define the reference distribution $\otimes_{n_k} \nu$ on \mathbb{R}^{n_k} , where n_k is the dimension of model k . The core idea is to learn approximate transport maps \hat{T}_k that map from the conditional posterior $\pi(\boldsymbol{\theta}_k | k)$ to the reference distribution. In practice, these maps are obtained by training normalizing flows on samples from $\pi(\boldsymbol{\theta}_k | k)$, minimizing the KL divergence between the push-forward of the base distribution and the target.

When proposing a move from model k to k' , the TRJ method constructs the trans-dimensional proposal as follows. First,

transform the current parameters to the reference space: $\mathbf{z}_k = T_k(\boldsymbol{\theta}_k)$. Then, apply a volume-preserving diffeomorphism $\bar{h}_{k,k'}$ that operates between reference spaces of different dimensions:

$$\mathbf{z}_{k'} = \bar{h}_{k,k'}(\mathbf{z}_k, \mathbf{u}_k),$$

where \mathbf{u}_k are auxiliary variables sampled from $\nu^{\otimes(n_{k'}-n_k)}$ to match dimensions when $n_{k'} > n_k$. Finally, the proposal in the target model space is obtained by inverting the transport map: $\boldsymbol{\theta}'_{k'} = T_{k'}^{-1}(\mathbf{z}_{k'})$.

A key theoretical result of [Davies et al. \(2023\)](#) establishes that when the transport maps exactly satisfy $T_{k\#}\pi_k = \otimes_{n_k}\nu$ for all $k \in \mathcal{K}$, the acceptance probability simplifies to:

$$\alpha(\mathbf{x}, \mathbf{x}') = 1 \wedge \frac{\pi(k')q(k | k')}{\pi(k)q(k' | k)},$$

which depends only on the model probabilities $\pi(k)$ and the model proposal distribution $q(\cdot | k)$. Furthermore, if the model proposals satisfy detailed balance with respect to the model probabilities ($\pi(k')q(k | k') = \pi(k)q(k' | k)$), the trans-dimensional moves become rejection-free.

2. VI with Normalizing Flows Transport RJMCMC

Variational inference with normalizing flows is an increasingly popular alternative to MCMC methods. Unlike the approach in the work of [Davies et al. \(2023\)](#), which learns transport map by using the forward KL divergence as a loss, in which samples from the conditional target distribution are generated by a pilot run of either MCMC, Sequential Monte Carlo samplers ([Moral et al., 2006](#)), or exact sampling, we adopt a more direct variational perspective. Our method does not require pre-sampling from the target distribution—a particular advantage when the conditional target is multi-modal with widely separated modes, or exhibits unfavorable geometry that hinders reliable exploration by standard MCMC algorithms. Instead, we work within the VI framework and minimize the reverse KL divergence, which only requires samples from a simple base distribution.

2.1. Variational Inference with Normalizing Flows

Variational inference minimizes the reverse KL divergence

$$\text{KL}(q_\eta \| p_*) = \mathbb{E}_{q_\eta} \left[\log \frac{q_\eta(\boldsymbol{\theta})}{p_*(\boldsymbol{\theta})} \right],$$

where q_η is the variational approximation with parameters η , and $p_*(\boldsymbol{\theta}) = \frac{p(\boldsymbol{\theta}, D)}{p(D)}$ is the posterior density given by Bayes' theorem. Here $p(\boldsymbol{\theta}, D)$ is the joint density of parameters $\boldsymbol{\theta} \in \mathbb{R}^d$ and data D , and $p(D)$ is the marginal likelihood.

Equivalently,

$$\text{KL}(q_\eta \| p_*) = \mathbb{E}_{q_\eta} \left[\log \frac{q_\eta(\boldsymbol{\theta})}{p(\boldsymbol{\theta}, D)} \right] + \log p(D).$$

A normalizing flow (NF) constructs a flexible approximation by transforming a base distribution q_0 through a smooth bijective map $f_\eta : \mathbb{R}^d \rightarrow \mathbb{R}^d$:

$$\mathbf{z} \sim q_0, \quad f_\eta(\mathbf{z}) \sim q_\eta.$$

The resulting density is

$$q_\eta(f_\eta(\mathbf{z})) = q_0(\mathbf{z}) |\det J_f(\mathbf{z})|^{-1},$$

where $J_f(\mathbf{z})$ is the Jacobian of f_η at \mathbf{z} .

Using the reparameterization trick ([Kingma & Welling, 2014](#)), the negative evidence lower bound (ELBO) can be written as

$$\mathbb{E}_{q_\eta} \left[\log \frac{q_\eta(\boldsymbol{\theta})}{p(\boldsymbol{\theta}, D)} \right] = \mathbb{E}_{q_0} \left[\log \frac{q_\eta(f_\eta(\mathbf{z}))}{p(f_\eta(\mathbf{z}), D)} \right].$$

Minimizing $\text{KL}(q_\eta \| p_*)$ requires computing the gradient

$$\nabla_\eta \text{KL}(q_\eta \| p_*) = \mathbb{E}_{q_0} \left[\nabla_\eta \log \frac{q_\eta(f_\eta(\mathbf{z}))}{p(f_\eta(\mathbf{z}), D)} \right].$$

Given samples $\{\mathbf{z}_k\}_{k=1}^b$ from q_0 , we estimate the gradient as

$$\nabla_\eta \text{KL}(q_\eta \| p_*) \approx \frac{1}{b} \sum_{k=1}^b \nabla_\eta \log \frac{q_\eta(f_\eta(\mathbf{z}_k))}{p(f_\eta(\mathbf{z}_k), D)}.$$

Alternatively, the lower-variance estimator proposed by [Roeder et al. \(2017\)](#) (often called path gradients) removes the score term:

$$\frac{1}{b} \sum_{k=1}^b \left[\nabla_\eta \log \frac{q_\eta(f_\eta(\mathbf{z}_k))}{p(f_\eta(\mathbf{z}_k), D)} - \nabla_\eta \log q_\eta(\boldsymbol{\theta}) \Big|_{\boldsymbol{\theta}=f_\eta(\mathbf{z}_k)} \right].$$

Scalable inference with normalizing flows requires invertible transformations with tractable Jacobian determinants. We highlight several methodological developments, detailed algorithmic descriptions are provided in Appendix. [Rezende & Mohamed \(2015\)](#) first introduced normalizing flows to variational inference, proposing planar and radial flows based on shallow MLPs. While computationally efficient, these early flows were limited by MLP expressivity. [Kingma et al. \(2016\)](#) developed Inverse Autoregressive Flows (IAF), which use autoregressive networks to produce triangular Jacobians, enabling expressive posteriors while maintaining computational efficiency. [Tomczak & Welling \(2016\)](#) proposed a volume-preserving flow based on Householder transformations, achieving competitive performance with improved numerical stability. Practical implementations have

been facilitated by packages such as normflows (Stimper et al., 2023), a PyTorch-based library supporting architectures including Real NVP (Dinh et al., 2017), Glow (Kingma & Dhariwal, 2018), and Neural Spline Flows (Durkan et al., 2019). Recent advances include stabilized training for high-dimensional affine coupling layers (Andrade, 2024) and annealing flows that combine continuous normalizing flows with dynamic optimal transport for multi-modal sampling in high dimensions (Wu & Xie, 2025).

2.2. Proposed Algorithm

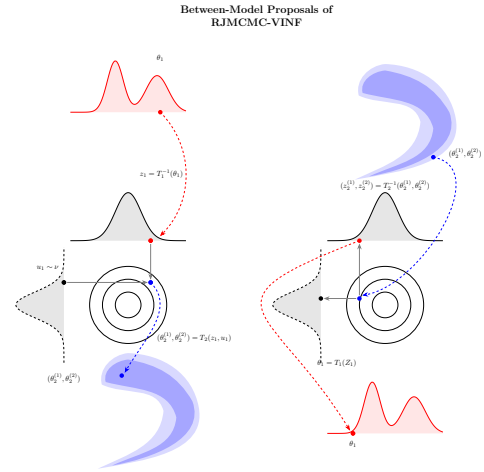
2.2.1. TRANSPORT REVERSIBLE JUMP MCMC WITH PROPOSALS DESIGNED BY VI WITH INDIVIDUAL NORMALIZING FLOWS

Our method proceeds as follows. First, we train approximate transport maps for each conditional posterior using variational inference with normalizing flows. Building upon recent advances in flow-based modeling (Stimper et al., 2023; Andrade, 2024), we incorporate transformation layers including RealNVP (Dinh et al., 2017), Neural Spline Flows (Durkan et al., 2019), and Masked Autoregressive Flow (Papamakarios et al., 2017). Parameter positivity is ensured via soft-plus transforms (Kucukelbir et al., 2017; Andrade, 2024). To better model heavy-tailed targets, we adopt a Student’s t base distribution (Andrade, 2024). The architecture composition adapts to specific target characteristics; training process follows Algorithm 1.

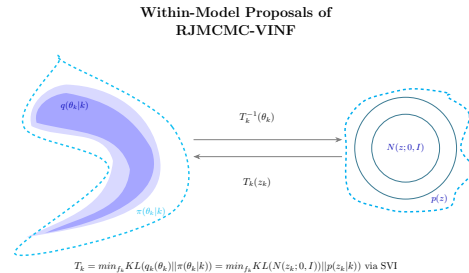
Algorithm 1 Stochastic Gradient Descent for VI with Normalizing Flows

- 1: $t \leftarrow 1; \ell^{(t)} \leftarrow \infty$
 - 2: Initialize $\eta^{(t)}$
 - 3: Initialize optimizer \mathcal{O} with global learning rate ξ_0
 - 4: **repeat**
 - 5: Sample $z_i \sim q_0$, for $i = 1, \dots, m$
 - 6: $g^{(t)} \leftarrow \frac{1}{b} \sum_{k=1}^b \left[\frac{\partial}{\partial \eta} \log \left(\frac{q_{\eta^{(t)}}(f_{\eta^{(t)}}(z_k))}{p(f_{\eta^{(t)}}(z_k), D)} \right) \right]$
 - 7: Find step size $\xi^{(t)}$ and direction $\Delta \eta^{(t)}$ with \mathcal{O} using $g^{(t)}$
 - 8: $\eta^{(t+1)} \leftarrow \eta^{(t)} + \xi^{(t)} \Delta \eta^{(t)}$
 - 9: $\ell^{(t+1)} \leftarrow \frac{1}{b} \sum_{k=1}^b \left[\log \left(\frac{q_{\eta^{(t+1)}}(f_{\eta^{(t+1)}}(z_k))}{p(f_{\eta^{(t+1)}}(z_k), D)} \right) \right]$
 - 10: $t \leftarrow t + 1$
 - 11: **until** $t > \text{max-iterations}$
-

Then, we design both between-model and within-model proposals based on the learned transport map, as illustrated in Figure 1. For the transport reversible jump proposal, we adopt the construction of Davies et al. (2023). Let $\otimes_{n_k} \nu$ denote the reference distribution; as a representative case, when $n_{k'} > n_k$, the trans-dimensional proposal in our pro-



(a) Between-Model Proposal using VI-NFs



(b) Within-Model Proposal using VI-NFs

Figure 1. Proposal mechanisms in RJMCMC-VINF: (a) transport reversible jump between models; (b) transport-enhanced moves within a model. Both are constructed using variational inference with normalizing flows, extending the approach of Davies et al. (2023); Hoffman et al. (2019).

posed algorithm proceeds as follows:

$$\begin{aligned} z_k &\leftarrow T_k^{-1}(\theta_k), \\ z'_{k'} &\leftarrow \bar{h}_{k,k'}(z_k, \mathbf{u}_k), \\ \theta_{k'} &\leftarrow T_{k'}(z'_{k'}), \end{aligned}$$

where \mathbf{u}_k denotes auxiliary variables drawn from ν to match dimensions and $\bar{h}_{k,k'}$ is typically set to the identity mapping (leading to simple concatenation or extraction of inputs), more structured choices are permissible. The complete between-model proposal construction is summarized in Algorithm 2.

For the within-model proposal, we draw inspiration from the ‘‘NeuTra’’ framework (Hoffman et al., 2019). Their approach employs inverse autoregressive flows (IAF) (Kingma et al., 2016) to approximate the transport map, and we note that inverting IAF transformations can be computationally expensive. Instead, we adopt Real-NVP (Dinh et al., 2017), which offers both fast sampling and efficient density evaluation. The NeuTra-style MCMC proceeds in three steps:

1. Fit a Real-NVP flow to learn an invertible transport map T by minimizing the reverse KL divergence from the variational approximate distribution $q(\theta) = q(z) \left| \frac{\partial T}{\partial z} \right|^{-1}$ to the target posterior $\pi(\theta)$.
2. Run a chosen MCMC algorithm in the latent z -space, targeting $\pi(z) = \pi(\theta = T(z)) \left| \partial T / \partial z \right|$, and initialize with a sample from $q(z)$.
3. Transform the z -samples via T to obtain samples from $\pi(\theta)$.

See Algorithm 3 for a detailed description.

A single iteration of the complete transport reversible jump MCMC procedure is outlined in Algorithm 4. In practice, this step is repeated for a specified number of iterations N , with the first B samples typically discarded as burn-in.

2.2.2. TRANS-DIMENSIONAL VARIATIONAL INFERENCE WITH CONDITIONAL NORMALIZING FLOWS

Rather than training a separate transport map for each model $k \in \mathcal{K}$, we extend the transport reversible jump (TRJ) framework (Davies et al., 2023) to trans-dimensional variational inference using conditional normalizing flows such that a conditional approximate transport map can be used. While Davies et al. (2025) employed inverse autoregressive flows (IAF) for trans-dimensional inference, we note that in the TRJ setting, both forward and inverse transformations must be computationally efficient. We therefore adopt RealNVP (coupling flows) (Dinh et al., 2017), which provides $O(1)$ complexity for both sampling and density evaluation while maintaining strong approximation capabilities: with flow

Algorithm 2 Between-Model Proposal of TRJ Designed by VI-NFs

Input: Current state $x = (k, \theta_k)$, target π , base density ν , transport maps $\{T_k\}_{k=1}^K$

Output: $x' = (k', \theta_{k'})$

- 1: $z_k \leftarrow T_k^{-1}(\theta_k)$
 - 2: **if** $n_{k'} > n_k$ **then**
 - 3: $w_k \leftarrow n_{k'} - n_k$
 - 4: **Draw** $u \sim \nu^{\otimes w_k}$
 - 5: $g_u \leftarrow \nu^{\otimes w_k}(u)$
 - 6: $g'_u \leftarrow 1$
 - 7: $z_{k'} \leftarrow \bar{h}_{k,k'}(z_k, u)$
 - 8: **else if** $n_{k'} < n_k$ **then**
 - 9: $w_{k'} \leftarrow n_k - n_{k'}$
 - 10: $(z_{k'}, u) \leftarrow \bar{h}_{k,k'}^{-1}(z_k)$
 - 11: $g_u \leftarrow 1$
 - 12: $g'_u \leftarrow \nu^{\otimes w_k}(u)$
 - 13: **else**
 - 14: $z_{k'} \leftarrow \bar{h}_{k,k'}^{-1}(z_k)$
 - 15: $g_u \leftarrow 1$
 - 16: $g'_u \leftarrow 1$
 - 17: **end if**
 - 18: $\theta'_{k'} \leftarrow T_{k'}(z_{k'})$
 - 19: $x' \leftarrow (k', \theta'_{k'})$
 - 20: $\alpha \leftarrow 1 \wedge \frac{\pi(x') j_{k'}(k) g'_u}{\pi(x) j_k(k') g_u} |J_{T_k}(\theta_k)|^{-1} |J_{T_{k'}}(\theta'_{k'})|$
 - 21: **Draw** $V \sim \mathcal{U}(0, 1)$
 - 22: **if** $\alpha > V$ **then**
 - 23: $x' \leftarrow x'$
 - 24: **else**
 - 25: $x' \leftarrow x$
 - 26: **end if**
-

Algorithm 3 Within-Model Proposal of TRJ Designed by VI-NFs

Input: Current state $x = (k, \theta_k)$, target $\{\pi_k\}$, transport maps $\{T_k\}_{k=1}^K$

Output: $x' = (k, \theta')$

- 1: Run a chosen MCMC algorithm in the latent z -space, targeting $\pi_k(z) = \pi(\theta = T_k(z)) \left| \partial T_k / \partial z \right|$, and initialize with a sample from $q(z)$.
 - 2: Transform the z -samples via T_k to obtain samples from $\pi_k(\theta)$.
-

length $r \geq 3$, RealNVP is theoretically sufficient for accurate approximation (Draxler et al., 2024; Koehler et al., 2021).

Following the dimension saturation approach of Davies et al. (2025), we define the augmented target distribution on the trans-dimensional support \mathcal{X} :

$$\tilde{\pi}(\tilde{x}) = \pi(x) \otimes \nu^{\otimes (n_{\max} - n_k)}(\mathbf{u}_{\sim k}),$$

where $n_{\max} = \max_{k \in \mathcal{K}} n_k$ is the maximum model di-

Algorithm 4 Transport RJMCMC with proposals generated by VI-NFs

Input: Current state $x = (k, \theta_k)$, target π , model proposal distribution $q(\cdot | k)$, between-model proposal $\{Q_{k \rightarrow k'}\}$, within-model kernels $\{P_k\}$

Output: x'

- 1: Train transport maps $\{T_k\}_{k=1}^K$ via Algorithm 1
- 2: Propose new model $k' \sim q(\cdot | k)$
- 3: **if** $k' = k$ **then**
- 4: Generate $\theta'_k \sim P_k(\theta_k, \cdot)$
- 5: $x' \leftarrow (k, \theta'_k)$
- 6: **else**
- 7: Generate $\theta'_{k'} \sim Q_{k \rightarrow k'}(\theta_k, \cdot)$
- 8: $x' \leftarrow (k', \theta'_{k'})$
- 9: **end if**

mension, $\tilde{x} = (k, \boldsymbol{\theta}_k, \mathbf{u}_{\sim k})$, and $\sim k$ identifies auxiliary variables of dimension $n_{\max} - n_k$. The saturated support $(\boldsymbol{\theta}_k, \mathbf{u}_{\sim k}) \in \Theta_k \times \mathcal{U}_k \subseteq \mathbb{R}^{n_{\max}}$ unifies the parameter space across models.

Defined on the same augmented support is the family of saturated variational densities

$$\tilde{q}_{\phi, \psi}(m, \boldsymbol{\theta}_m, \mathbf{u}_{\setminus m}) = \tilde{q}_{\phi}(\boldsymbol{\theta}_m, \mathbf{u}_{\setminus m} | m) q_{\psi}(m),$$

where, noting the availability of a transport $(\boldsymbol{\theta}_m, \mathbf{u}_{\setminus m}) = T_{\phi}(\mathbf{z} | m)$, $\mathbf{z} \in \mathcal{U}^{d_{\max}}$, we define the NFs

$$\begin{aligned} \tilde{q}_{\phi}(\boldsymbol{\theta}_m, \mathbf{u}_{\setminus m} | m) &:= \nu_{d_{\max}}(T_{\phi}^{-1}(\boldsymbol{\theta}_m, \mathbf{u}_{\setminus m} | m)) \\ &\quad \times \left| \det \nabla T_{\phi}^{-1}(\boldsymbol{\theta}_m, \mathbf{u}_{\setminus m} | m) \right|, \\ &= \nu_{d_{\max}}(\mathbf{z}) \left| \det \nabla T_{\phi}(\mathbf{z} | m) \right|^{-1}. \end{aligned}$$

Our goal is to construct the real-NVP so that variational approximate distribution can factorize into model parameters and *i.i.d.* auxiliary parts, i.e.

$$\tilde{q}_{\phi}(\boldsymbol{\theta}_m, \mathbf{u}_{\setminus m} | m) = q_{\phi}(\boldsymbol{\theta}_m | m) \nu_{d_{\setminus m}}(\mathbf{u}_{\setminus m}).$$

The core challenge is to design a conditional normalizing flow that factorizes into model parameters and auxiliary parts based on the model indicator k . Let $A_k : \{1, \dots, n_{\max}\} \rightarrow \{0, 1\}$ indicate whether coordinate i is active in model k . We define a binary mask $\mathbf{m}_k \in \{0, 1\}^{n_{\max}}$ where $m_{k,i} = A_k(i)$. For RealNVP coupling layers (Dinh et al., 2017), we modify the scaling and translation functions to be conditionally dependent on both the parameter values and model indicator:

$$\mathbf{z}_{1:d} = \mathbf{x}_{1:d}$$

$$\mathbf{z}_{d+1:n_{\max}} = \mathbf{x}_{d+1:n_{\max}} \odot \exp(s_{\phi}(\mathbf{x}_{1:d}, k)) + t_{\phi}(\mathbf{x}_{1:d}, k),$$

where s_{ϕ} and t_{ϕ} are neural networks that take the model indicator k as additional input via a context network. In

this setting, one can obtain approximate TMs by training a single conditional VI with NFs with the conditioning vector being the model index $k \in \mathcal{K}$. Then the associated proposal are constructed as $\mathcal{C}_{k,k'} = c_{k'} \circ T_{\phi}(\cdot | k') \circ T_{\phi}^{-1}(\cdot | k) \circ c_k$, where $k' \sim j_k$, and c_k is simply concatenation. This yields TRJ with VI with conditional normalizing flows. (Further details are provided in the supplement.)

2.2.3. MARGINAL LIKELIHOOD ESTIMATION VIA REAL-NVP

Real-NVP offers computational advantages through fast sampling and density evaluation, enabling efficient marginal likelihood estimation via importance sampling:

$$p(D) = \mathbb{E}_{q_{\eta}} \left[\frac{p(\theta, D)}{q_{\eta}(\theta)} \right] \approx \frac{1}{b_{\text{eval}}} \sum_{k=1}^{b_{\text{eval}}} \frac{p(\theta_k, D)}{q_{\eta}(\theta_k)}, \quad (1)$$

where $\theta_k \sim q_{\eta}$ for $k = 1, \dots, b_{\text{eval}}$ (Andrade, 2024).

These estimates, obtained concurrently during normalizing flow training, serve dual purposes: (1) computing Bayes factors for model comparison, and (2) informing the model proposal distribution $q(k)$ within the reversible jump framework. The transport reversible jump (TRJ) proposal (Davies et al., 2023) exhibits the desirable property that the acceptance probability depends solely on the model probabilities. Furthermore, variational inference with normalizing flows can achieve substantially sharper estimates of marginal likelihoods compared to SMC (Moral et al., 2006), as demonstrated in the experiments of Andrade (2024).

3. Numerical Experiments

MCMC Diagnoses. To assess the performance of a RJMCMC sampler, we monitor the running estimates of the posterior model probabilities. Faster mixing chains are expected to yield more reliable estimates with fewer iterations, providing a practical diagnostic for convergence and sampler efficiency.

Bartolucci Bridge Estimator. To ensure consistent benchmarking with the methodology of Davies et al. (2023), we employ the same Bartolucci bridge estimator (BBE) for model probability assessment. The BBE, derived from Rao-Blackwellized bridge sampling (Bartolucci et al., 2006), constructs Bayes factor estimates between models k and k' as:

$$\hat{B}_{k,k'} = \frac{N_{k'}^{-1} \sum_{i=1}^{N_{k'}} \alpha'_i}{N_k^{-1} \sum_{i=1}^{N_k} \alpha_i}, \quad (2)$$

where $N_k, N_{k'}$ count proposals between models, and α_i, α'_i are corresponding acceptance probabilities. Under uniform model priors, it is straightforward to convert estimators

of Bayes factors to estimators of model probabilities (Bartolucci et al., 2006) via

$$\hat{\pi}(k) = \hat{B}_{jk}^{-1} \left(1 + \sum_{i \in \mathcal{K} \setminus \{j\}} \hat{B}_{i,j} \right)^{-1} \quad (3)$$

for arbitrary $j \in \mathcal{K}$. The BBE serves as a low-variance diagnostic for comparing proposal mechanisms when applied to identical sample sets and fixed model-jump probabilities. We compute BBE using an independent evaluation set of N samples per model, generating one RJMCMC proposal per sample to obtain the acceptance probabilities required for Eq. (2).

3.1. Illustrative Example

3.1.1. MODEL SETUP

Consider a two-model trans-dimensional target constructed via pushforward of a Gaussian through a known parametric nonlinear map, we use the (element-wise) inverse sinh-arcsinh (SAS) transformation of Jones & Pewsey (2009),

$$S_{\epsilon, \delta}(x) = \sinh(\delta^{-1} \odot (\sinh^{-1}(x) + \epsilon))$$

where $\epsilon \in \mathcal{R}^n$ and $\delta \in \mathcal{R}_+^n$.

Define a transformation

$$T(Z) = S_{\epsilon, \delta}(LZ)$$

for an $n \times n$ matrix L , where $Z \sim \mathcal{N}(0_n, I_n)$. Then the induced density for the transformed variable $\theta = T(Z)$ is

$$p_{\epsilon, \delta, L}(\theta) = \phi_{LL^\top}(S_{\epsilon, \delta}^{-1}(\theta)) |J_{S_{\epsilon, \delta}^{-1}}(\theta)|,$$

with inverse transform $S_{\epsilon, \delta}^{-1}(y) = \sinh(\delta \odot \sinh^{-1}(y) - \epsilon)$.

We construct a two-model trans-dimensional target with dimensions $n_1 = 1$ and $n_2 = 2$. Let the prior model probabilities be $\frac{1}{4}$ for model 1 and $\frac{3}{4}$ for model 2. The joint target distribution is then

$$\pi(k, \theta_k) = \begin{cases} \frac{1}{4} p_{\epsilon_1, \delta_1, 1}(\theta_1), & k = 1, \\ \frac{3}{4} p_{\epsilon_2, \delta_2, L}(\theta_2), & k = 2, \end{cases}$$

where

$$\epsilon_1 = -2, \quad \delta_1 = 1, \quad \epsilon_2 = (1.5, -2), \quad \delta_2 = (1, 1.5),$$

and L is the Cholesky factor satisfying

$$LL^\top = \begin{bmatrix} 1 & 0.99 \\ 0.99 & 1 \end{bmatrix}.$$

3.1.2. EXPERIMENTAL RESULTS

Following Davies et al. (2023), we train both affine and masked autoregressive transforms with rational quadratic splines (RQMA-NF) (Durkan et al., 2019) on $N = 5 \times 10^4$ exact simulation samples per target. For our proposed VI-NFs method, we employ planar flows (Rezende & Mohamed, 2015) and Real-NVP (Dinh et al., 2017) as approximate distributions for the 1D and 2D targets, respectively.

Figure 2 visualizes proposal distributions under each method, including the exact transport map baseline. Our transport reversible jump proposals designed by VI-NFs generates proposals that closely align with the exact map, substantially outperforming both RQMA-NF and affine approximations. Correspondingly, Figure 3 shows that VI-NFs achieve the most accurate and stable running estimates of model probabilities after the exact map, with consistently lower variance than alternative approximations. The RQMA-NF and affine methods exhibit higher variability and slower convergence, as reflected in their proposal distributions' deviation from the exact transport.

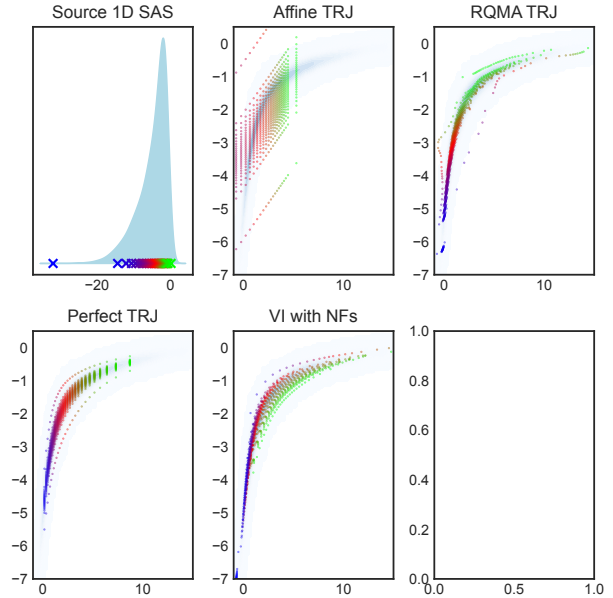


Figure 2. Visualization of trans-dimensional proposals for the Sinh-Arcsinh target. Systematic draws from $\pi(x_1|k=1)$ are transported from the 1D model ($k=1$) to the 2D model ($k=2$) via: (a) approximate affine, (b) RQMA-NF, (c) exact transport map, and (d) our VI-NFs (Real-NVP). Auxiliary variables are sampled systematically (30 per source point).

3.2. Bayesian Factor Analysis Example

3.2.1. MODEL SETUP

Considering a Bayesian Factor Analysis Example, we model monthly exchange rates of six currencies relative

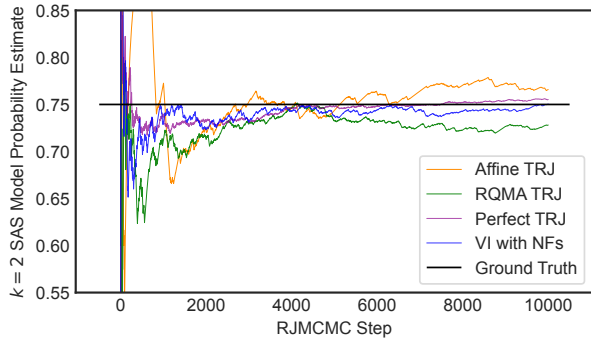


Figure 3. Convergence diagnostics for Sinh-Arcsinh model probabilities. Running estimates of $P(k = 2|y)$ are shown for each proposal type: Affine, RQMA-NF, exact map, and VI-NFs (Real-NVP). Within-model proposals alternate with simple Gaussian random walks.

to the British pound, spanning January 1975 to December 1986 (Lopes & West, 2004), denoted as $y_i \in \mathcal{R}^6$ for $i = 1, \dots, 143$, of the random vector \mathbf{Y} . We assume that the observed data Y follows a multivariate normal distribution with mean zero and covariance matrix Σ . Specifically, $Y \sim \mathcal{N}(\mathbf{0}_6, \Sigma)$, where the covariance matrix is structured as $\Sigma = \beta_k \beta_k^\top + \Lambda$ and Λ is a 6×6 positive diagonal matrix, β_k is a $6 \times k$ lower-triangular matrix with strictly positive diagonal entries, k denotes the number of latent factors, and the corresponding parameter vector θ_k has dimension $6(k + 1) - k(k - 1)/2$.

Following the model configuration in the work of Davies et al. (2023); Lopes & West (2004), we assign the following priors to the elements of $\beta_k = [\beta_{ij}]$, where $i = 1, \dots, 6$ and $j = 1, \dots, k$:

$$\begin{aligned} \beta_{ij} &\sim \mathcal{N}(0, 1), & i > j, \\ \beta_{jj} &\sim \mathcal{N}_+(0, 1), \\ \Lambda_{ii} &\sim \mathcal{IG}(1.1, 0.05). \end{aligned}$$

Our primary interest lies in the joint posterior distribution of the model index k and the parameters $\theta_k = (\beta_k, \Lambda)$ for $k = 2$ or 3 factors, corresponding to parameter dimensions 17 and 21, respectively. By Bayes’ theorem, this posterior is proportional to

$$\pi(k, \theta_k | y) \propto p(k) p(\beta_k | k) p(\Lambda) \prod_{i=1}^{143} \phi_{\beta\beta^\top + \Lambda}(y_i),$$

where $y = (y_1, \dots, y_{143})$ denotes the full dataset of 143 observations.

3.2.2. EXPERIMENT RESULTS

Factor Analysis Experimental Setup We evaluate three trans-dimensional proposal methods: (1) the independence

RJMCMC sampler of Lopes & West (2004) as baseline, (2) the transport reversible jump (TRJ) approach of Davies et al. (2023) with normalizing flows pre-trained with samples from the conditional targets, and (3) our proposed VI-NFs method integrating variational inference with Real-NVP (Dinh et al., 2017) as the approximate distribution. Parameter positivity is enforced via softplus transforms (Kucukelbir et al., 2017; Andrade, 2024).

Following Davies et al. (2023), we employ No-U-Turn Sampler (NUTS) (Hoffman & Gelman, 2014) implemented in PyMC (Salvatier et al., 2016) for inference in the three-factor model, and static temperature-annealed sequential Monte Carlo (SMC) (Moral et al., 2006) for the two-factor model. For each configuration, we maintain equal-sized training and evaluation sets, considering both $N = 2 \times 10^3$ and $N = 1.6 \times 10^4$ samples per model to assess sensitivity to sample size.

Figure 4 compares the convergence of posterior model probability estimates for the two-factor model across three proposal methods: the baseline independence sampler (Lopes & West, 2004), the RQMA-NF transport proposal, and our VI-NFs approach. Ground truth (0.88) is indicated as a horizontal line. Each chain performed 10^5 MCMC steps with alternating trans-dimensional and within-model random walk proposals. Our VI-NFs method achieves both faster convergence and lower variance than the baseline, while RQMA-NF shows intermediate performance with reduced stability compared to VI-NFs.

Figure 5 visualizes proposal distributions in selected bivariate marginal spaces, contrasting each method against a ground-truth kernel density estimate from 5×10^4 SMC particles. The independent sampler exhibits significant deviation from the target structure, while transport-based methods better preserve the target geometry. Among these, VI-NFs most closely approximates the ground truth, demonstrating its effectiveness in constructing accurate trans-dimensional proposals.

3.3. Variable Selection in Robust Regression Example

Our final example addresses block variable selection within a robust regression framework (Davies et al., 2023). We observe a response Y that depends linearly on predictors X_1, X_2, X_3 via the model

$$Y = \beta_0 + \beta_1 X_1 + \beta_2 X_2 + \beta_3 X_3 + \varepsilon,$$

where the error term ε is modeled as a mixture of a standard normal and a normal distribution with large variance, i.e. $\mathcal{N}(0, 10^2)$, thereby introducing robustness to outliers.

The model space is indexed by a binary vector $k = (k_1, k_2)$, with $k_i \in \{0, 1\}$ indicating whether predictor block i is included. Therefore there is a model space of cardinality of

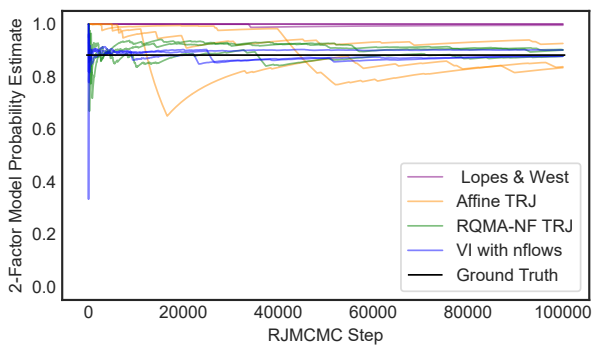


Figure 4. Running estimates of the model probabilities for the two-factor model. Proposal types are the (Lopes & West, 2004) independence proposal, Affine and RQMA-NF proposals using Algorithm 1 and Variational Inference with Real-NVP using Algorithm 2. Five chains on each proposal type are depicted, where alternating withinmodel proposals are not shown.

4, composed of all models of the form $k = (1, k_1, k_2, k_2)$ where $k_i \in \{0, 1\}$ for $i = 1, 2$. We adopt the following prior specification:

$$k_i \sim \text{Bernoulli}\left(\frac{1}{2}\right), \quad i = 1, 2,$$

$$\beta_i \sim \mathcal{N}(0, 10^2), \quad i = 0, 1, 2, 3.$$

The target distribution π is the joint posterior over the discrete model indicators k and the continuous regression coefficients $\beta = (\beta_0, \dots, \beta_3)$, obtained via Bayes’ theorem.

3.3.1. EXPERIMENT RESULTS

We simulate data from a linear model with active predictors corresponding to $k = (1, 1, 0, 0)$ and parameters $\theta_k = (\beta_0, \beta_1)$. To induce multimodal posterior structure, response observations are equally split between configurations $(\beta_0, \beta_1) = (1, 1)$ and $(6, 1)$. The design matrix entries are i.i.d. $\mathcal{N}(0, 1)$, with residuals $\epsilon \sim \mathcal{N}(0, 25)$.

Five proposal mechanisms are compared: (1) *Standard*: independence auxiliary sampler (Brooks et al., 2003) using prior $\mathcal{N}(0, 10^2)$ as ν ; (2) *TRJ-Affine*: affine transport maps via Algorithm 1 of Davies et al. (2023); (3) *TRJ-ROMA-NF*: ROMA-NF transport maps via the same algorithm 1 of Davies et al. (2023); (4) *CTRJ*: conditional normalizing flow approach (Algorithm 2 of Davies et al. (2023)); (5) *VI-NFs*: our proposed method integrating variational inference with Real-NVP in TRJ.

Evaluation employs the Bartolucci bridge estimator (BBE) on matched training/evaluation sets ($N \in \{500, 4000\}$ from a single SMC run), with 80 independent trials to assess variability.

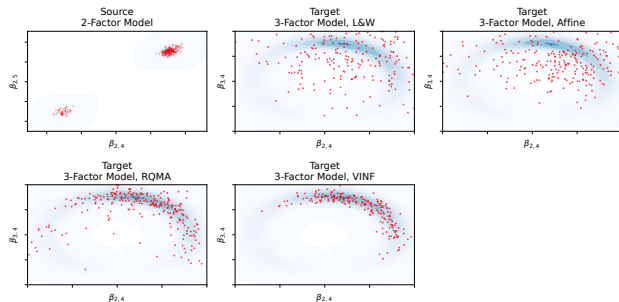


Figure 5. A visualization (using selected bivariate plots) of the proposal from points on the 2-factor model (top-left) to proposed points on the 3-factor model for each proposal type:(Lopes & West, 2004) independence RJMCMC proposal (top middle); TRJ with Affine map (top right); TRJ with RQMA-NF map (bottom left) and TRJ with VI-NFs (bottom middle). Ground truth kernel density estimate was made using 5×10^4 SMC particles from (South et al., 2019).

Variability Analysis Results Figure 6 compares the distribution of model probability estimates across all five proposal types. Three key observations emerge: (1) All transport-based methods (TRJ-Affine, TRJ-ROMA-NF, CTRJ, and VI-NFs) significantly outperform the standard independence sampler in both accuracy and stability; (2) Among transport methods, VI-NFs achieves the lowest variance and closest alignment with the SMC ground truth; (3) Conditional approaches (CTRJ and VI-NFs) match or exceed the performance of their individual-flow counterparts while requiring only a single flow architecture, offering substantial efficiency gains. Notably, VI-NFs demonstrates the better overall balance of accuracy and stability, with its distribution tightly concentrated around the ground truth value. This suggests that integrating variational inference with normalizing flows provides a robust mechanism for constructing effective trans-dimensional proposals, particularly in multimodal settings where exact transport maps are unavailable.

References

Andrade, D. Stabilizing training of affine coupling layers for high-dimensional variational inference. *Machine Learning: Science and Technology*, 5(4):045066, 2024. doi: 10.1088/2632-2153/ad9a39.

Bartolucci, F., Scaccia, L., and Mira, A. Efficient bayes factor estimation from the reversible jump output. *Biometrika*, 93(1):41–52, 2006. doi: 10.1093/biomet/93.1.41.

Blei, D. M., Kucukelbir, A., and McAuliffe, J. D. Variational inference: A review for statisticians. *Journal of the American Statistical Association*, 112(518):859–877, 2017. doi: 10.1080/01621459.2017.1285773.

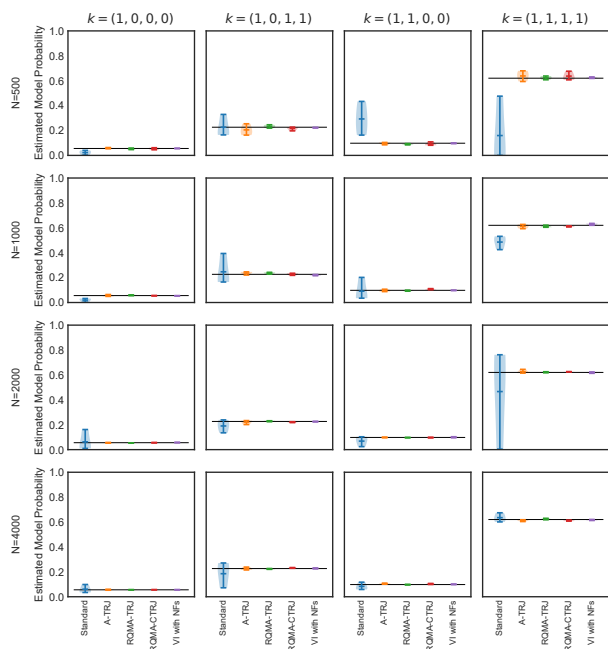


Figure 6. Violin plot showing the variability of the k model probability estimate for each proposal type using the Bartolucci Estimator vs a ground truth given by individual SMC ($N = 5 \times 10^4$). Here, Indiv RQMA-NF TRJ corresponds to Algorithm 1 of (Davies et al., 2023) with Affine and RQMA individual normalizing flows, whereas RQMA-CNF TRJ corresponds to Algorithm 2 of (Davies et al., 2023) using a single conditional normalizing flow, VI-NFs corresponds to using VI with Real-NVP to design transport Reversible jump proposal.

Brooks, S. P., Giudici, P., and Roberts, G. O. Efficient construction of reversible jump markov chain monte carlo proposal distributions. *Journal of the Royal Statistical Society: Series B*, 65(1):3–39, 2003. doi: 10.1111/1467-9868.03711.

Davies, L., Salomone, R., Sutton, M., and Drovandi, C. Transport reversible jump proposals. In *Proceedings of the 26th International Conference on Artificial Intelligence and Statistics*, pp. 6839–6852, 2023. URL <https://proceedings.mlr.press/v206/davies23a.html>.

Davies, L., Mackinlay, D., Oliveira, R., and Sisson, S. A. Amortized variational transdimensional inference. In *Advances in Neural Information Processing Systems*, 2025. URL <https://neurips.cc/virtual/2025/loc/san-diego/poster/118604>.

Dinh, L., Sohl-Dickstein, J., and Bengio, S. Density estimation using real NVP. In *International Conference on Learning Representations*, 2017. URL <https://openreview.net/forum?id=HkpbH9lx>.

Draxler, F., Wahl, S., Schnörr, C., and Köthe, U. On the universality of volume-preserving and coupling-based normalizing flows. In *Proceedings of the 41st International Conference on Machine Learning*, pp. 11613–11641, 2024. URL <https://proceedings.mlr.press/v235/draxler24a.html>.

Durkan, C., Bekasov, A., Murray, I., and Papamakarios, G. Neural spline flows. In *Advances in Neural Information Processing Systems*, pp. 7511–7522, 2019. URL https://proceedings.neurips.cc/paper_files/paper/2019/hash/7ac71d433f282034e088473244df8c02-Abstract.html.

Durkan, C., Bekasov, A., Murray, I., and Papamakarios, G. nflows: Normalizing flows in PyTorch. *Zenodo*, 2020. URL <https://doi.org/10.5281/zenodo.4296287>.

Fan, Y., Peters, G. W., and Sisson, S. A. Automating and evaluating reversible jump MCMC proposal distributions. *Statistics and Computing*, 19(4):409–421, 2009. doi: 10.1007/s11222-008-9101-z.

Gabrié, M., Rotskoff, G. M., and Vanden-Eijnden, E. Efficient Bayesian sampling using normalizing flows to assist Markov chain Monte Carlo methods. In *ICML Workshop on Invertible Neural Networks, Normalizing Flows, and Explicit Likelihood Models*, 2021. URL <https://openreview.net/forum?id=mvtoohBjOwx>.

Gagnon, P. Informed reversible jump algorithms. *Electronic Journal of Statistics*, 15(2), 2021. doi: 10.1214/21-EJS1877.

GREEN, P. J. Reversible jump markov chain monte carlo computation and bayesian model determination. *Biometrika*, 82(4):711–732, 1995. doi: 10.1093/biomet/82.4.711.

Green, P. J. and Mira, A. Delayed rejection in reversible jump Metropolis–Hastings. *Biometrika*, 88(4):1035–1053, 2001. doi: 10.1093/biomet/88.4.1035.

Hastings, W. K. Monte carlo sampling methods using markov chains and their applications. *Biometrika*, 57(1):97–109, 1970. doi: 10.1093/biomet/57.1.97.

Hoffman, M., Sountsov, P., Dillon, J. V., Langmore, I., Tran, D., and Vasudevan, S. NeuTra-lizing bad geometry in hamiltonian monte carlo using neural transport, 2019. URL <http://arxiv.org/abs/1903.03704>.

Hoffman, M. D. and Gelman, A. The no-U-turn sampler: Adaptively setting path lengths in hamiltonian monte carlo. *Journal of Machine Learning Research*, 15(47):1593–1623, 2014. URL <https://jmlr.org/papers/v15/hoffman14a.html>.

- Jasra, A., Stephens, D. A., and Holmes, C. C. Population-based reversible jump markov chain monte carlo. *Biometrika*, 94(4):787–807, 2007. doi: 10.1093/biomet/asm069.
- Jiao, X., Flouri, T., and Yang, Z. Multispecies coalescent and its applications to infer species phylogenies and cross-species gene flow. *National Science Review*, 8(12):nwab127, 2021. doi: 10.1093/nsr/nwab127.
- Jones, M. C. and Pewsey, A. Sinh-arcsinh distributions. *Biometrika*, 96(4):761–780, 2009. doi: 10.1093/biomet/asp053.
- Karagiannis, G. and Andrieu, C. Annealed importance sampling reversible jump MCMC algorithms. *Journal of Computational and Graphical Statistics*, 22(3):623–648, 2013. doi: 10.1080/10618600.2013.805651.
- Kingma, D. P. and Dhariwal, P. Glow: Generative flow with invertible 1x1 convolutions. In *Advances in Neural Information Processing Systems*, pp. 10215–10224, 2018. URL https://proceedings.neurips.cc/paper_files/paper/2018/hash/d139db6a236200b21cc7f752979132d0-Abstract.html.
- Kingma, D. P. and Welling, M. Auto-encoding variational bayes. In *The 2nd International Conference on Learning Representations*, 2014. URL <https://arxiv.org/abs/1312.6114>.
- Kingma, D. P., Salimans, T., and Welling, M. Improving variational inference with inverse autoregressive flow. In *Advances in Neural Information Processing Systems*, pp. 4743–4751, 2016. URL https://proceedings.neurips.cc/paper_files/paper/2016/hash/ddeebdeefdb7e7e7a697e1c3e3d8ef54-Abstract.html.
- Koehler, F., Mehta, V., and Risteski, A. Representational aspects of depth and conditioning in normalizing flows. In *Proceedings of the 38th International Conference on Machine Learning*, pp. 5628–5636, 2021. URL <https://proceedings.mlr.press/v139/koehler21a.html>.
- Kucukelbir, A., Tran, D., Ranganath, R., Gelman, A., and Blei, D. M. Automatic differentiation variational inference. *Journal of Machine Learning Research*, 18(14):1–45, 2017. URL <http://jmlr.org/papers/v18/16-107.html>.
- Lopes, H. F. and West, M. Bayesian model assessment in factor analysis. *Statistica Sinica*, 14(1):41–67, 2004. URL <https://www3.stat.sinica.edu.tw/statistica/j14n1/j14n12/j14n12.html>.
- Marzouk, Y., Moselhy, T., Parno, M., and Spantini, A. Sampling via measure transport: An introduction. In Ghanem, R., Higdon, D., and Owhadi, H. (eds.), *Handbook of Uncertainty Quantification*, pp. 1–41. Springer International Publishing, Cham, 2016. doi: 10.1007/978-3-319-11259-6_23-1.
- Moral, P. D., Doucet, A., and Jasra, A. Sequential monte carlo samplers. *Journal of the Royal Statistical Society: Series B*, 68(3):411–436, 2006. doi: 10.1111/j.1467-9868.2006.00553.x.
- Neal, R. M. MCMC using Hamiltonian dynamics. In *Handbook of Markov Chain Monte Carlo*, pp. 113–162. Chapman and Hall/CRC, 2011. URL <https://www.taylorfrancis.com/chapters/edit/10.1201/b10905-6>.
- Papamakarios, G., Pavlakou, T., and Murray, I. Masked autoregressive flow for density estimation. In *Advances in Neural Information Processing Systems*, pp. 2338–2347, 2017. URL https://proceedings.neurips.cc/paper_files/paper/2017/hash/6c1da886822c67822bcf3679d04369fa-Abstract.html.
- Papamakarios, G., Nalisnick, E., Rezende, D. J., Mohamed, S., and Lakshminarayanan, B. Normalizing flows for probabilistic modeling and inference. *Journal of Machine Learning Research*, 22(57):1–64, 2021. URL <https://jmlr.org/papers/v22/19-1028.html>.
- Parno, M. D. and Marzouk, Y. M. Transport map accelerated markov chain monte carlo. *SIAM/ASA Journal on Uncertainty Quantification*, 6(2):645–682, 2018. doi: 10.1137/17M1134640.
- Pravitasari, A. A., Hermanto, Y. P., Iriawan, N., Irhamah, Fithriasari, K., Purnami, S. W., and Ferriastuti, W. MRI-based brain tumor segmentation using gaussian mixture model with reversible jump markov chain monte carlo algorithm. In *The 2nd International Conference on Science, Mathematics, Environment, and Education*, pp. 020085, 2019. doi: 10.1063/1.5139817.
- Rezende, D. and Mohamed, S. Variational inference with normalizing flows. In *Proceedings of the 32nd International Conference on Machine Learning*, pp. 1530–1538, 2015. URL <https://proceedings.mlr.press/v37/rezende15.html>.
- Roeder, G., Wu, Y., and Duvenaud, D. K. Sticking the landing: Simple, lower-variance gradient estimators for variational inference. In *Advances in Neural Information Processing Systems*, pp. 6925–6934, 2017. URL https://proceedings.neurips.cc/paper_files/paper/2017/hash/

e91068fff3d7fa1594dfdf3b4308433a-Abstract.html.

Salvatier, J., Wiecki, T. V., and Fonnesbeck, C. Probabilistic programming in python using PyMC3. *PeerJ Computer Science*, 2:e55, 2016. doi: 10.7717/peerj-cs.55.

South, L. F., Pettitt, A. N., and Drovandi, C. C. Sequential monte carlo samplers with independent markov chain monte carlo proposals. *Bayesian Analysis*, 14(3), 2019. doi: 10.1214/18-BA1129.

Stimper, V., Liu, D., Campbell, A., Berenz, V., Ryll, L., Schölkopf, B., and Hernández-Lobato, J. M. Normflows: A PyTorch package for NormalizingFlows. *Journal of Open Source Software*, 8(86):5361, 2023. doi: 10.21105/joss.05361.

Tomczak, J. M. and Welling, M. Improving variational auto-encoders using householder flow. In *NIPS Workshop on Bayesian Deep Learning*, 2016. URL <https://arxiv.org/abs/1611.09630>.

Wu, D. and Xie, Y. Annealing flow generative models towards sampling high-dimensional and multi-modal distributions. In *Forty-Second International Conference on Machine Learning*, 2025. URL <https://icml.cc/virtual/2025/poster/44357>.